Docosahexaenoic and Eicosapentaenoic Acids Segregate Differently between Raft and Nonraft Domains

Justin A. Williams,[†] Shawn E. Batten,[†] Mitchel Harris,[‡§] Benjamin Drew Rockett,[‡§] Saame Raza Shaikh,[‡§] William Stillwell,[¶] and Stephen R. Wassall[†*]

[†]Department of Physics, Indiana University-Purdue University Indianapolis, Indianapolis, Indiana; [‡]Department of Biochemistry and Molecular Biology and [§]East Carolina Diabetes and Obesity Institute, East Carolina University, Greenville, North Carolina; and [¶]Department of Biology, Indiana University-Purdue University Indianapolis, Indianapolis, Indiana

ABSTRACT Omega-3 polyunsaturated fatty acids (n-3 PUFA), enriched in fish oils, are increasingly recognized to have potential benefits for treating many human afflictions. Despite the importance of PUFA, their molecular mechanism of action remains unclear. One emerging hypothesis is that phospholipids containing n-3 PUFA acyl chains modify the structure and composition of membrane rafts, thus affecting cell signaling. In this study the two major n-3 PUFA found in fish oils, eicosapentaenoic (EPA) and docosahexaenoic (DHA) acids, are compared. Using solid-state ^{2}H NMR spectroscopy we explored the molecular organization of 1-[$^2H_{31}$]palmitoyl-2-eicosapentaenoylphosphatidylcholine (PEPC-d_{31}) and 1-[$^2H_{31}$]palmitoyl-2-docosahexaenoylphosphatidylcholine (PDPC-d_{31}) in mixtures with sphingomyelin (SM) and cholesterol (chol). Our results indicate that whereas both PEPC-d_{31} and PDPC-d_{31} can accumulate into SM-rich/chol-rich raftlike domains, the tendency for DHA to incorporate into rafts is more than twice as great as for EPA. We propose that DHA may be the more bioactive component of fish oil that serves to disrupt lipid raft domain organization. This mechanism represents an evolution in the view of how PUFA remodel membrane architecture.

INTRODUCTION

Fish oil supplements are increasingly recognized in clinical studies to have utility in treating a variety of important human afflictions (1–4). However, the molecular mode of action of fish oil remains unclear. The major bioactive components of fish oil are the long-chain ω-3 polyunsaturated fatty acids (n-3 PUFA) eicosapentaenoic (EPA, 20:5$\Delta^{5,8,11,14,17}$) and docosahexaenoic (DHA, 22:6$\Delta^{4,7,10,13,16,19}$) acids. Omega-3 fatty acids are characterized by having their last double-bond three carbons from the terminal methyl (n or ω) end of the chain. One emerging mechanism of action for n-3 PUFA is modification of membrane organization in response to uptake of EPA and/or DHA into phospholipids of the cellular plasma membrane (5–7).

It is now generally accepted that lipids are not randomly distributed within a membrane. They are laterally arranged in patches or domains of specific composition that provide the environment necessary for the function of resident proteins (8). Differential lipid-lipid and lipid-protein affinity drives the formation of the domains. The best-known example is the lipid raft (9,10). Lipid rafts are liquid-ordered (l_o) domains enriched in saturated sphingolipids and cholesterol (chol) that serve as the platform for characteristic signaling proteins. The extended conformation adopted by the saturated acyl chains of sphingolipids is compatible with close proximity to the four rigid cycloalkane rings of the sterol, while hydrogen bonding of the amide on the sphingosine backbone of a sphingolipid molecule to the hydroxyl of adjacent sphingolipid and chol molecules glues the raft together (11). By contrast, the shallow energy barrier to rotation about C-C bonds in the repeating =C-C-C= unit in a PUFA chain produces a multitude of rapidly changing conformations (12,13) that push chol away, as evinced by reduced solubility (14) and binding coefficients (15) measured for the sterol in polyunsaturated phospholipids.

We have hypothesized from work on model membranes that poor affinity of chol for PUFA promotes formation of membrane (nonraft) domains rich in PUFA-containing phospholipids but poor in chol (16–19). According to our hypothesis, highly disordered PUFA-rich domains coexist in a sea of bulk lipid with highly ordered lipid rafts that are enriched in sphingolipids and chol (6,20). A recent refinement to this view, based on detergent extraction (21,22) and microscopy studies of living cells (22,23), has polyunsaturated phospholipids infiltrating rafts as well as forming (nonraft) domains (7,24). In either case, the basic model is that n-3 PUFA modulate membrane organization to diminish intracellular or extracellular signaling events.

Mixtures of polyunsaturated phospholipids with sphingomyelin (SM) and chol are the model membrane system that we have developed to investigate the sorting of lipids into SM-rich/chol-rich raftlike domains and PUFA-rich/chol-poor nonraft domains (6,20). DHA, the most unsaturated fatty acid commonly found in nature (25), was the focus of our earlier work. In a series of studies we employed solid-state ^{2}H NMR spectroscopy, together with a battery of complementary biophysical techniques, to characterize 1-palmitoyl-2-docosahexaenoylphosphatidylethanolamine

Submitted November 9, 2011, and accepted for publication June 12, 2012.

*Correspondence: swassall@iupui.edu

Editor: Klaus Gawrisch.

0006-3495/12/07/0228/10 $2.00

http://dx.doi.org/10.1016/j.bpj.2012.06.016

(PDPE)/SM/chol (1:1:1 mol) membranes (16–18). The NMR spectra established the presence of motionally distinct DHA-rich/chol-poor (less-ordered) and SM-rich/chol-rich (more-ordered) domains that are nanoscale in size. Here we turn our attention to EPA, which is typically more abundant than DHA in fish oil capsules (26) and differs in its efficacy in treating certain ailments (27–29).

We specifically address whether EPA and DHA interact differentially with SM and chol. Utilizing solid-state ^{2}H NMR, the molecular organization of 1-[$^2H_{31}$]palmitoyl-2-eicosapentaenoylphosphatidylcholine (PEPC-d_{31}), 1-[$^2H_{31}$]palmitoyl-2-docosahexaenoylphosphatidylcholine (PDPC-d_{31}) and, as a control, 1-[$^2H_{31}$]palmitoyl-2-oleoylphosphatidylcholine (POPC-d_{31}) were compared in mixtures with SM (1:1 mol) and with SM and chol (1:1:1 mol). Fig. 1 depicts the molecular structure of the phospholipids and sphingolipid studied. The ^{2}H NMR data establish that the two major bioactive components of fish oil do not exert the same effect on membrane organization. EPA segregates into PUFA-rich/chol-poor (nonraft) domains more than DHA. Strikingly, contrary to our earlier model, our experiments reveal that a substantial amount of the DHA-containing phospholipid incorporates into SM-rich/chol-rich (raft) domains. The observation that n-3 PUFA can infiltrate raft-like domains in a lipid mixture is consistent with recent studies in vitro and in vivo showing n-3 PUFA can incorporate into detergent-resistant membranes (DRM) (7).

MATERIALS AND METHODS

Solid-state ^{2}H NMR of model membranes

Materials

Avanti Polar Lipids (Alabaster, AL) was the source for POPC-d_{31}, PEPC-d_{31}, PDPC-d_{31}, and egg SM as either a stock item or custom synthesis. Chol was purchased from Sigma Chemical (St. Louis, MO). All lipids were used without further purification. Deuterium-depleted water was obtained from Cambridge Isotope Laboratories (Andover, MA).

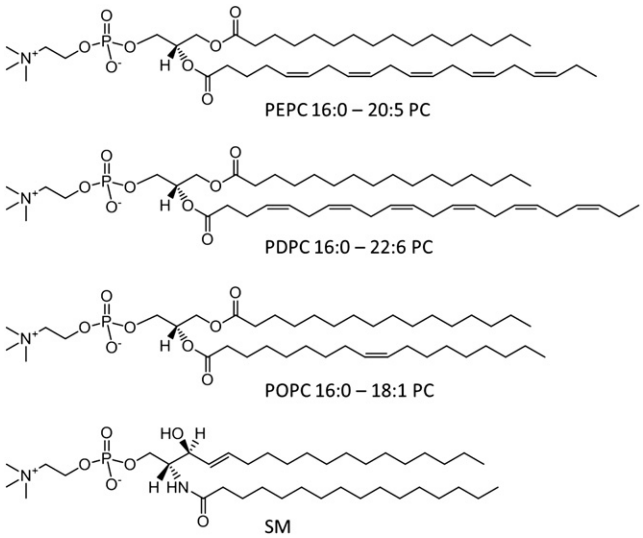

FIGURE 1 Molecular structure of PEPC, PDPC, POPC, and SM.

Sample preparation

Lipids mixtures containing ~50 mg total lipid were codissolved in chloroform in molar ratio 1:1 and 1:1:1, respectively, for deuterated PC/SM and deuterated PC/SM/chol samples (concentrations that will be assumed henceforth unless otherwise specified). The chloroform was evaporated under a steady stream of argon, and the samples were placed in vacuum overnight to remove any remaining solvent. After adding 50 wt % degassed 50 mM Tris buffer to the dried lipids, the samples were vortex-mixed and pH was adjusted to 7.5 in the presence of additional water. Three lyophilizations with deuterium-depleted water were then performed to remove trace amounts of natural abundance ^{2}HHO, and finally the lipids were hydrated at 50 wt %. In each instance, hydration was performed above 45°C, which exceeds the gel-to-liquid-crystalline temperature for SM that has the highest chain-melting temperature (39°C) (30), to ensure proper mixing. Samples were packed and sealed in 5-mm glass NMR tubes, stored at −80°C and equilibrated at room temperature before experiments. Precautions were taken throughout the procedure to minimize oxidation (16), including limiting exposure to light and using a glove box purged with argon during manipulations.

Spectroscopy

Solid-state ^{2}H NMR spectra were acquired on a home-built spectrometer (31) operating at 46.0 MHz with a 7.05 T super-conducting magnet (Oxford Instruments, Osney Mead, UK). Pulse programming was accomplished with an in-house assembled programmable pulse generator, while signals were obtained in quadrature using a dual-channel digital oscilloscope (R1200 M; Rapid Systems, Seattle, WA). Sample temperature was regulated to ±0.5°C by a temperature controller (1600 Series; Love Controls, Michigan City, IN). To eliminate spectral distortion due to receiver recovery time, a phase-alternated quadrupolar echo sequence $(90°_x\text{-}\tau\text{-}90°_y\text{-acquire-delay})_n$ was implemented (32). Parameters were 90° pulse width ≈3 μs; separation between pulses $\tau = 50$ μs; delay between pulse sequences = 1.0 s (gel phase) or 1.5 s (liquid-crystalline phase); sweep width = ±250 kHz (gel phase) or ±100 kHz (liquid-crystalline phase); dataset = 2 K; and number of transients = 2048 (gel phase) or 1536 (liquid-crystalline phase).

Spectral analysis

First moments M_1 were calculated from ^{2}H-NMR spectra according to

$$M_1 = \frac{\int_{-\infty}^{\infty} |\omega| f(\omega) d\omega}{\int_{-\infty}^{\infty} f(\omega) d\omega}, \quad (1)$$

where ω is the frequency with respect to the central Larmor frequency and $f(\omega)$ is the lineshape (33). In practice, the integral was a summation over the digitized data. The expression

$$M_1 = \frac{\pi}{\sqrt{3}} \left(\frac{e^2 qQ}{h} \right) |\overline{S}_{CD}| \quad (2)$$

was employed in the lamellar liquid-crystalline phase to relate the first moment M_1 to the average order parameter $\overline{S}_{CD}$ for the perdeuterated palmitoyl *sn*-1 chain via the static quadrupolar coupling constant $(e^2qQ/h) = 167$ kHz. A reproducibility of ±2% typically applies to the M_1 values measured.

Spectra were also fast-Fourier-transform (FFT) dePaked to enhance resolution in the liquid-crystalline phase (34). This numerical procedure generates a spectrum representative of a planar membrane of single alignment from the powder pattern signal. In processing the intrinsically noisy dePaked data, the out-of-phase channel was zeroed before Fourier transformation. The resultant spectra were reflected about the central frequency and possess an improvement in signal/noise by a factor of $\sqrt{2}$.

RESULTS

Solid-state ^{2}H NMR of model membranes

Solid-state ^{2}H NMR spectra were obtained for 50 wt % aqueous multilamellar suspensions of PEPC-d_{31}, PDPC-d_{31}, and POPC-d_{31} in mixtures with SM, and with SM and chol. The perdeuterated palmitoyl (16:0) *sn*-1 chain of the PC molecules constitutes an essentially noninvasive probe and the spectra compared the molecular organization of EPA-containing PC versus DHA-containing PC in the mixed membranes. Oleic acid (OA)-containing PC acted as a monounsaturated control. The experiments were conducted from high-to-low temperature over a range from 40 to −32°C that encompasses the gel-to-liquid-crystalline phase transition for each lipid. Representative spectra can be seen in Fig. 2.

PC/SM mixtures

At low temperature, −24°C, the spectra for PEPC-d_{31}, PDPC-d_{31}, and POPC-d_{31} in the mixtures with SM are symptomatic of the gel phase (Fig. 2, *a–c*). They appear broad and relatively featureless with edges at ±63 kHz reflecting the slow rotational diffusion of the all-*trans* palmitic acid chain that renders the lineshape nonaxially symmetric (asymmetry parameter $\eta \neq 0$) (33). By contrast at high temperature, 37°C, the lineshape in each case is characteristic of phospholipids in the lamellar liquid-crystalline phase (Fig. 2, *d–f*). A superposition of powder patterns from all of the individual deuterated positions along the perdeuterated palmitoyl *sn*-1 chain produces a spectrum with well-defined edges at ±~12 kHz corresponding to the plateau region of nearly constant order in the upper portion of the chain and a series of pairs of peaks within the spectrum associated with less-ordered methylenes and the terminal methyl in the lower portion of the chain (33). Greater disorder and a shorter plateau region are indicated for the PUFA-containing phospholipids by the slightly narrower width and lower intensity of the edges seen for PEPC-d_{31} (Fig. 2 *d*) and PDPC-d_{31} (Fig. 2 *e*) relative to POPC-d_{31} (Fig. 2 *f*).

The spectra presented in Fig. 2 illustrate the tremendous change in lineshape that accompanies the melting of lipid chains at the gel-to-liquid-crystalline phase transition. The first moment (M_1), defined in Eq. 1, offers a way to quantify lineshape and provides a means to investigate phase behavior when plotted as a function of temperature. Fig. 3 shows the dependence on temperature for the values of M_1 calculated from the spectra collected for PEPC-d_{31}, PDPC-d_{31}, and POPC-d_{31} in the mixtures with SM between −32 and 40°C. An abrupt drop signifying the transition from gel ($M_1 > 1.3 \times 10^5$ s^{-1}) to liquid-crystalline ($M_1 < 0.6 \times 10^5$ s^{-1}) state is seen with each mixture (Fig. 3 *A*). The midpoint temperature (designated as the transition temperature T_m) and width of this drop in value for the moment are, respectively, −16 and 5°C for PEPC-d_{31} and −14 and 6°C for PDPC-d_{31}, as opposed to −3 and 18°C for POPC-d_{31}.

An appraisal of data obtained with the corresponding pure PC membranes establishes that the transition observed in the mixed membranes with SM is broadened but hardly shifted in temperature, and that the broadening is much smaller with polyunsaturated than monounsaturated phospholipid. For PDPC-d_{31}, $T_m = -12.7$°C (35), and for POPC-d_{31}, $T_m = -6$°C (36), and in both cases the transition is relatively narrow (2–3°C in width). Although to the best of our knowledge details of the phase behavior have not been published for PEPC, differential scanning calorimetry measurements on pure PC bilayers with stearic (18:0) acid at the *sn*-1 position and a series of unsaturated fatty acids at the *sn*-2 position indicate T_m is slightly lower (3–4°C) with EPA than DHA (37).

The modest impact upon the temperature of the phase transition seen here for PEPC-d_{31}, PDPC-d_{31}, and POPC-d_{31} in the presence of SM indicates that the mixing of PC and SM is inhomogeneous, which we attribute to segregation into PC-rich and SM-rich domains. A similar interpretation has previously been applied to ^{2}H NMR spectra recorded for POPC/SM mixtures (11,38,39). Other studies on PEPC/SM or PDPC/SM mixtures have not been published. The appreciably smaller SM-associated effect on the width of the phase transition for PEPC-d_{31} and PDPC-d_{31} in relation to POPC-d_{31} (Fig. 3 *A*) we ascribe to enhanced separation between the PUFA-containing phospholipids and sphingolipid compared to the OA-containing phospholipid and sphingolipid.

PC/SM/chol mixtures

In Fig. 2 (*lower panel*), spectra for PEPC-d_{31}, PDPC-d_{31}, and POPC-d_{31} in mixtures with SM and chol are plotted. All three systems exhibit a spectrum that is gel-like in appearance at −24°C (Fig. 2, *g–i*). There is a reduction in intensity in the wings compared to the spectra collected under identical conditions in the absence of chol (Fig. 2, *a–c*). The implication is that the sterol disrupts the regular packing of the chains of PEPC-d_{31}, PDPC-d_{31}, and POPC-d_{31} in the mixed membranes in the gel state. The spectra observed in the liquid-crystalline state at 37°C reveal a remarkable differential in the response of each PC to the introduction of chol into the mixed PC/SM systems (Fig. 2, *j–l*). A spectrum that is similar in shape to POPC-d_{31}/SM (Fig. 2 *f*), but appreciably broader with edges at ±20 kHz, is seen with POPC-d_{31}/SM/chol (Fig. 2 *l*). This

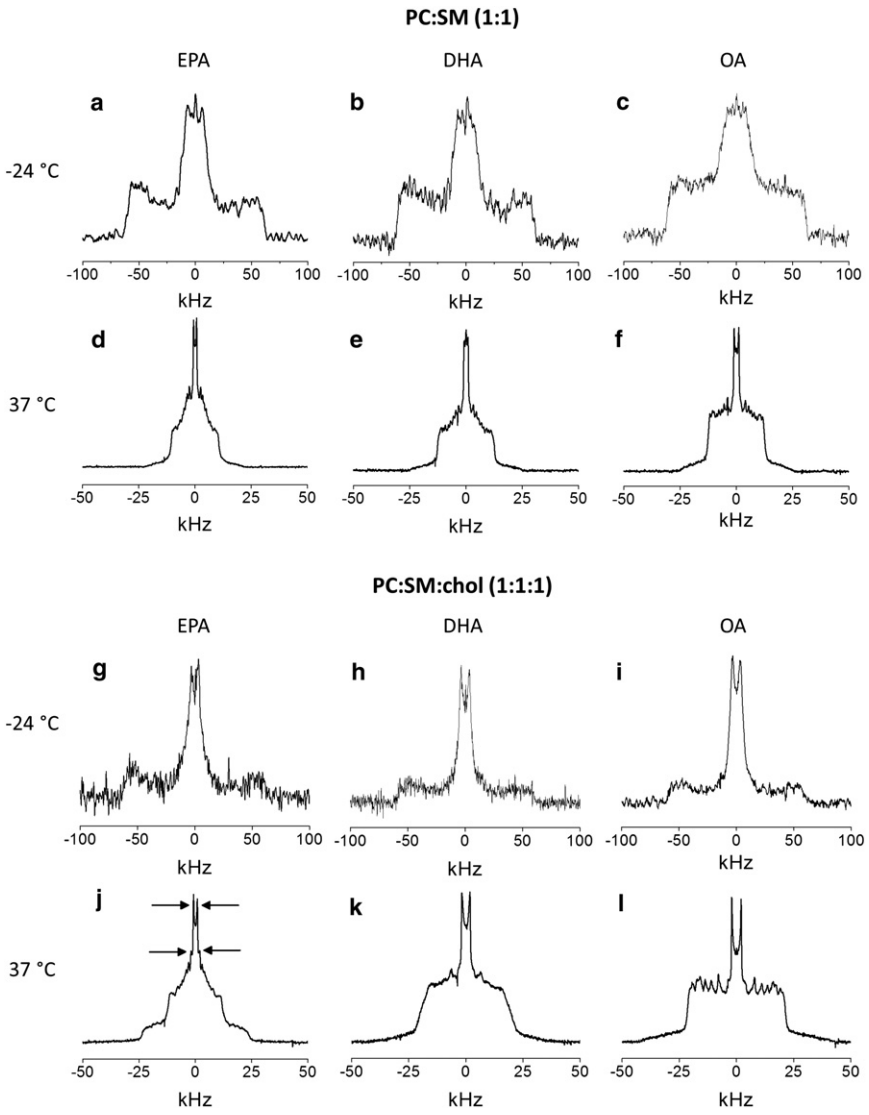

FIGURE 2 ^{2}H NMR spectra for 50 wt % aqueous dispersions in 50 mM Tris buffer (pH 7.5) of PEPC-d_{31}/SM (1:1 mol) (*a* and *d*), PDPC-d_{31}/SM (1:1 mol) (*b* and *e*), and POPC-d_{31}/SM (1:1 mol) (*c* and *f*) (*upper panel*), and PEPC-d_{31}/SM/chol (1:1:1 mol) (*g* and *j*), PDPC-d_{31}/SM/chol (1:1:1 mol) (*h* and *k*), and POPC-d_{31}/SM/chol (1:1:1 mol) (*i* and *l*) (*lower panel*). Spectra were recorded at −24 (*upper row*) and 37°C (*lower row*). (*Arrows*, *j*) Signals assigned to the terminal methyl group on PEPC-d_{31} in PC-rich (inner-splitting) and SM-rich (outer-splitting) domains (see Fig. S2).

broadening reflects the restriction to chain motion caused by the rigid steroid ring moiety.

The addition of chol to the mixtures containing PUFA and SM elicits a more profound alteration in spectral shape. In the spectrum for PEPC-d_{31}/SM/chol (Fig. 2 *j*), a narrow component with edges at ±12 kHz closely resembling that seen in the absence of sterol (Fig. 2 *d*) appears superposed upon a wider second spectral component with edges at ±23 kHz. The distinction is less dramatic in the case of the system containing DHA where a second spectral component is not discernible (Fig. 2 *k*). Instead, the spectrum for PDPC-d_{31}/SM/chol is smeared-out with less sharply defined edges at ±19 kHz and barely resolved peaks, except for the central pair due to the terminal methyl group. Interpretation of the spectra collected at 37°C in terms of the sorting of lipids into PC-rich and SM-rich domains that is amplified when chol is present to different extent by EPA and DHA will be given later in the Discussion.

Fig. 3 *B* shows the variation with temperature of the first moment evaluated for PEPC-d_{31}, PDPC-d_{31}, and POPC-d_{31} in the mixtures with SM and chol. A clear distinction is apparent in the effect that the sterol has on the phase behavior of EPA- versus DHA- and OA-containing phospholipid in the mixtures with SM. The value of M_1 for POPC-d_{31}/SM/chol slowly decreases with increasing temperature and a discontinuity is no longer observed. The introduction of chol into the POPC-d_{31}/SM membrane broadens the phase transition for POPC-d_{31} beyond detection, indicating extensive mixing of chol and POPC-d_{31}. PDPC-d_{31} responds comparably. The moments that were measured for PDPC-d_{31}/SM/chol similarly decline gradually and without break as temperature rises. In dramatic contrast, much less thorough mixing of chol with PEPC-d_{31} is indicated in PEPC-d_{31}/SM/chol. A sharp fall in first moment (from $M_1 \sim 1.4 \times 10^5$ to ~0.6×10^5 s^{-1}) still occurs, but is somewhat reduced in magnitude and (with midpoint ~−18°C and width ~12°C) less precipitous compared to

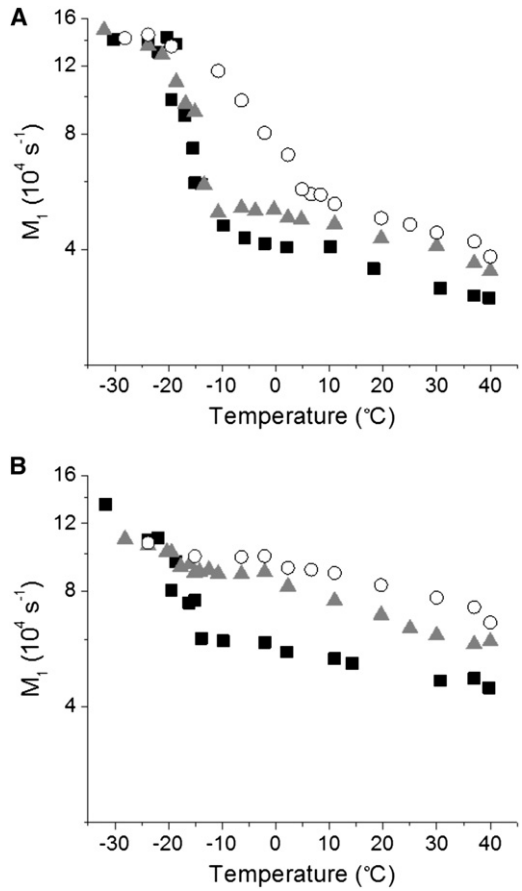

FIGURE 3 Variation of the first moment M_1 derived from ^{2}H NMR spectra as a function of temperature for PEPC-d_{31}/SM (1:1 mol) (■), PDPC-d_{31}/SM (1:1 mol) (▲), and POPC-d_{31}/SM (1:1 mol) (○) in the absence (*A*) and presence (*B*) of chol (1:1:1 mol).

PEPC-d_{31}/SM (Fig. 3 *A*). Unlike not only POPC-d_{31}, but also PDPC-d_{31}, adding chol does not totally obliterate the phase transition for PEPC-d_{31} in the mixed membrane.

We surmise from the temperature variation of the spectra seen here for PEPC-d_{31}, PDPC-d_{31}, and POPC-d_{31} in 1:1 mol mixtures with SM and in 1:1:1 mol mixtures with SM and chol that the lipids incompletely mix to form PC-rich and SM-rich domains. Notably, a lower affinity of sterol for EPA than DHA and thereby a greater propensity for DHA-containing PC than EPA-containing PC to incorporate into SM-rich/chol-rich raftlike domains are implied. It should be noted that the two-domain model invoked does not rule out more complex phase behavior.

Detergent extraction of cells

To complement our experiments on model membranes, we explored the incorporation of EPA and DHA into biological membranes. Details of the methods are provided in the Supporting Material. The uptake of EPA versus DHA, relative to a bovine serum albumin control, into DRM (raft) and detergent-soluble membranes (DSM) (nonraft) fractions isolated from EL4 cells by detergent extraction is compared in Fig. S1 in the Supporting Material. EPA constituted ~2% (not statistically significant, $p = 0.05$) and ~11% of the total fatty acid, respectively, found in DRM (*upper panel*) and DSM (*lower panel*) after treatment with EPA, whereas DHA constituted ~6% and ~33% of the total fatty acid found in DRM and DSM, respectively, after treatment with DHA. It is important to note that elevated levels of docosapentaenoic (DPA, 22:5n-3) acid, the elongation product of EPA (40), were detected in DRM (~6%) and DSM (~23%) when the cells were treated with EPA. The combined concentration of EPA+DPA approximately matches the uptake measured for DHA in each fraction (i.e., the total level of n-3 PUFA is roughly the same after treatment with EPA and DHA).

DISCUSSION

The n-3 PUFA found in fish oils alleviate the symptoms associated with a multitude of inflammatory, autoimmune, and metabolic diseases (1–4). The diversity of the health benefits suggests an underlying general mechanism. We (5–7), and other research groups (21,23,41), have hypothesized that changes in molecular organization within the plasma membrane due to the incorporation of n-3 PUFA into phospholipids modulate the conformation, and thereby the activity, of signaling proteins. The formation of highly disordered domains that are enriched in DHA-containing phospholipids but depleted in chol is a model that we developed based on studies on lipid bilayers (6,20). These nonraft domains form because the rapidly varying conformers adopted by PUFA are averse to near approach to the rigid steroid moiety of the sterol. An alternative model in which, paradoxically, PUFA-containing phospholipids invade and disrupt the highly ordered environment existing within lipid rafts that are enriched in predominantly saturated chain sphingolipids and chol has recently been developed based on in-vitro and in-vivo studies (7,24). Central to the formulation of this model was the significant amount of DHA detected in DRM isolated from cells treated with PUFA.

In this investigation, we employed solid-state ^{2}H NMR to compare the molecular organization of an EPA- and DHA-containing phospholipid in mixtures with the lipid raft molecules SM and chol. EPA, with 20 carbons and five double bonds, and DHA, with 22 carbons and six double bonds, are the n-3 PUFA present in fish oils. Our experiments on model membranes demonstrate a significant difference in the partitioning of EPA and DHA between raft and nonraft domains, and reveal that n-3 PUFA can accumulate in raftlike domains.

Segregation into PC-rich (nonraft) and SM-rich (raft) domains

We interpret the ^{2}H NMR spectra for PEPC-d_{31}, PDPC-d_{31} and POPC-d_{31} mixed with SM (Fig. 2, *upper panel*) in terms

of segregation into PC-rich and SM-rich domains. The precipitous drop in value of the first moment derived from the spectra as a function of temperature that accompanies chain melting indicates in each instance that the transition from gel to liquid-crystalline state is broadened and only minimally shifted in temperature due to the presence of SM (Fig. 3 *A*). Inhomogeneous mixing of PC and SM is implied.

A marked differential in the response of EPA and DHA to the addition of chol is revealed by the ^{2}H NMR spectra for PEPC-d_{31}, PDPC-d_{31}, and POPC-d_{31} in the mixtures with SM and chol (Fig. 2, *lower panel*). Substantial exposure to chol is inferred for PDPC-d_{31} from the absence of a discontinuity in the temperature dependence of the moments derived from spectra (Fig. 3 *B*). A phase transition from gel to liquid-crystalline state for PDPC-d_{31} is no longer discernible in PDPC-d_{31}/SM/chol because chol disturbs the packing and obstructs reorientation of the DHA-containing phospholipid in the gel and liquid-crystalline states, respectively. This behavior resembles that observed with POPC-d_{31} in our POPC-d_{31}/SM/chol control (Fig. 3 *B*) and POPC-d_{31}/SM/chol mixtures of similar composition (11,8,39). There is, on the contrary, still an abrupt drop in the plot of moment against temperature for PEPC-d_{31} in PEPC-d_{31}/SM/chol (Fig. 3 *B*). Less interaction with the sterol, so that a phase transition remains, is implied for the EPA-containing phospholipid compared to its DHA-containing counterpart when mixed with SM and chol.

Further insight is gleaned from the average order parameter $\overline{S}_{CD}$, the correspondence of which to bilayer thickness underscores the physical significance (42), calculated via Eq. 2 from the first moment M_1 for spectra at 37°C (see Table S1 in the Supporting Material). The values of $\overline{S}_{CD}$ in PC/SM mixtures where chol was absent are lower for PEPC-d_{31} ($\overline{S}_{CD} = 0.100$) and PDPC-$d_{31}$ ($\overline{S}_{CD} = 0.122$) than POPC-$d_{31}$ ($\overline{S}_{CD} = 0.137$), confirming our qualitative assessment of the spectra. They show, moreover, that EPA-containing PC is more disordered than DHA-containing PC in combination with SM. Consistent with demixing into PC-rich and SM-rich domains that produces a population-weighted average value for $\overline{S}_{CD}$ from the two domains, comparison with previously published data on POPC-d_{31} (36) and PDPC-d_{31} (43) indicates there is only a small (little more than experimental uncertainty) increase due to SM. No data for PEPC-d_{31} were found in a search of the literature.

After the addition of chol to the PC/SM mixed membranes, $\overline{S}_{CD}$ is increased in every case. The increase is greatest with POPC-d_{31} ($\Delta\overline{S}_{CD} = 0.094$) and, reflecting the poor affinity chol has for highly disordered PUFA (20), is more modest with PEPC-d_{31} ($\Delta\overline{S}_{CD} = 0.056$) and PDPC-$d_{31}$ ($\Delta\overline{S}_{CD} = 0.070$). Based on the hierarchy of the changes in $\overline{S}_{CD}$ measured, we infer that the sterol is pushed out of PC-rich domains into SM-rich domains by EPA > DHA > OA. Here it is assumed that a given concentration of chol exerts an equivalent ordering effect upon PEPC-d_{31}, PDPC-d_{31}, and POPC-d_{31} individually. This assumption is supported by spectra published for [$^2H_{35}$]stearoyl-2-oleoylphosphatidylcholine (SOPC-d_{35}) (44) and [$^2H_{35}$]stearoyl-2-docosahexaenoylphosphatidylcholine (SDPC-d_{35}) (45) and by spectral moments reported for POPC-d_{31} (46) and [$^2H_{31}$]palmitoyl-2-arachidonoylphosphatidylcholine (PAPC-d_{31}) (47) that suggest the *sn*-1 chain in the monounsaturated and polyunsaturated systems responds comparably to chol.

Domain size is increased with PUFA

The variation in appearance of the spectra for PEPC-d_{31}/SM/chol, PDPC-d_{31}/SM/chol, and POPC-d_{31}/SM/chol at 37°C (Fig. 2, *lower panel*) implies that the size of domains is enlarged by EPA and DHA with respect to OA. That only a single spectral component was observed in the spectrum for POPC-d_{31}/SM/chol (Fig. 2 *l*), we ascribe to incomplete demixing into PC-rich (less-ordered) and SM-rich (more-ordered) domains between which there is fast exchange (48). A time-averaged spectrum, rather than a superposition of spectral components, is produced because POPC-d_{31} moves among domains at a rate that exceeds the difference in splitting for spectra from the two domains. Invoking the difference in splitting ($\Delta\nu = 1600$ Hz) previously reported for the terminal methyl groups on POPC-d_{31} and [$^2H_{31}$]-N-palmitoylsphingomyelin (PSM-d_{31}) in a PC/SM/chol (3:3:2 mol) mixture of similar composition (38) as representative of PC-rich and SM-rich domains, the lifetime for the residency of lipid molecules in a domain must be less than $\tau = (2\pi\Delta\nu)^{-1} = 9.9 \times 10^{-5}$ s. The exchange of lipids between domains is presumed to be mediated by lateral diffusion with $D \sim 5 \times 10^{-12}$ m^2 s^{-1} (49) so that the root-mean displacement $r = (4D\tau)^{1/2}$ associated with the lifetime places an upper limit of <45 nm upon the radius of domains.

Slow exchange at a rate less than the difference in splitting for spectra due to PEPC-d_{31} in PC-rich and SM-rich domains, in contrast, applies to PEPC-d_{31}/SM/chol (Fig. 2 *j*). The result is observation of a superposition of individual spectral components from the two domains. There is a narrow spectral component with edges at ± 12 kHz (less-ordered PC-rich/chol-poor domains) superposed upon a wider second component with edges at ± 23 kHz (more-ordered SM-rich/chol-rich domains). The difference in splitting ($\Delta\nu = 2800$ Hz) for the terminal methyl groups on PEPC-d_{31} in the two domains (highlighted by *arrows* and see Fig. S2) then, by an analogous calculation to that outlined above, corresponds to a lifetime for residency in a domain that must exceed $\tau = 5.7 \times 10^{-5}$ s and places a lower limit of >35 nm on the size.

A second spectral component is not discernible in the spectrum for PDPC-d_{31}/SM/chol (Fig. 2 *k*). Instead, a broadened spectrum in which individual peaks are smeared out was observed. We attribute this blurring of spectral features to exchange between domains on an intermediate timescale that is comparable to the difference in splitting

for PDPC-d_{31} in PC-rich and SM-rich domains. A domain size that falls between the ballpark estimates determined based on the extremes for fast and slow exchange in the OA- and EPA-containing systems is the likely explanation. Thus, we deduce that domains are larger with EPA and DHA relative to OA in PC/SM/chol-mixed membranes. The effect is also more marked for EPA than DHA. We emphasize that the splitting for the terminal methyl group employed in our calculations is sensitive to exchange on the timescale of the residual quadrupolar coupling associated with a rapidly rotating methyl group and that the estimates for domain size constitute upper or lower limits.

A PUFA-induced increase in the size of domains was not evident in our earlier work comparing PDPE with POPE (17,18). ^{2}H NMR spectra recorded for 1-[$^2H_{31}$] palmitoyl-2-oleoylphosphatidylethanolamine (POPE-d_{31}), 1-[$^2H_{31}$]palmitoyl-2-docosahexaenoylphosphatidylethanolamine (PDPE-d_{31}) and PSM-d_{31} in PE/SM (1:1 mol) and PE/SM/chol (1:1:1 mol) mixtures were consistent with the DHA-containing phospholipid, as well as the OA-containing phospholipid, undergoing fast exchange between PE-rich and SM-rich domains. The spectra for not only POPE-d_{31}, but also PDPE-d_{31}, remained well resolved upon the addition of chol. There was neither a smearing-out of spectral features nor the appearance of a second spectral component. An upper limit of $<$20 nm, moreover, was placed upon domain size (18). That, unlike PDPC-rich domains, an increase in size is not implied for PDPE-rich domains in the presence of the sterol we attribute to headgroup structure. The smaller PE headgroup and hydrogen-bonding to adjacent polar groups produce negative stress curvature that drives a tendency to adopt inverted hexagonal H_{II} phase that is enhanced with increasing level of unsaturation (50). Liquid-crystalline PDPE becomes inverted hexagonal at ~13°C and is lamellar over only a very narrow temperature range (6–10°C). This inherent instability of the PDPE bilayer may serve to restrict the area of PDPE-rich domains relative to PDPC-rich domains.

PUFA infiltrate rafts

An estimate of the amount of EPA- and DHA-containing phospholipids that incorporates into SM-rich/chol-rich raft-like domains can be made from the spectra for PEPC-d_{31}/SM/chol and PDPC-d_{31}/SM/chol at 30°C displayed in Fig. 4. The spectrum for PEPC-d_{31}/SM/chol (Fig. 4 *a*, *left*) closely resembles the spectrum at 37°C (Fig. 2 *j*). It is a superposition of narrow and broad components that, as at the higher temperature, we attribute to PEPC-d_{31} in PC-rich and SM-rich domains, respectively. However, the spectra for PDPC-d_{31}/SM/chol at 30 (Fig. 4 *b*, *left*) and 37°C (Fig. 2 *k*) differ. A pair of peaks (indicated by *arrows* and see Fig. S3) that coalesces into a single peak on going up in temperature is visible in the spectrum acquired at the lower temperature. We assign them to the terminal

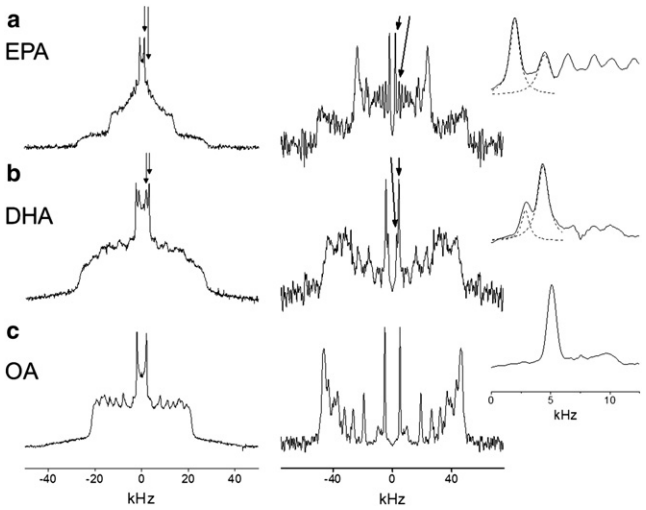

FIGURE 4 ^{2}H NMR spectra for PEPC-d_{31}/SM/chol (1:1:1 mol) (*a*), PDPC-d_{31}/SM/chol (1:1:1 mol) (*b*), and POPC-d_{31}/SM/chol (1:1:1 mol) (*c*) at 30°C. Standard FFT (powder pattern) spectra are plotted (*left column*); FFT dePaked (aligned) spectra are also plotted (*right column*). Peaks from signals assigned to the terminal methyl group on PEPC-d_{31} (*a*) and PDPC-d_{31} (*b*) in PC-rich (inner splitting) and SM-rich (outer splitting) domains are designated (*arrows*), whereas there is only a single peak for the terminal methyl group on POPC-d_{31} (*c*) (see Fig. S3 and Fig. S4). (*Insets*) Blow-up of these peaks (*dashed lines* are a Lorentzian fit). The signals are symmetric in frequency about the center of the spectra and only the peaks to the right of center with positive frequency are labeled.

methyl groups of PDPC-d_{31} in less-ordered PC-rich (inner-peak) and more-ordered SM-rich (outer-peak) domains. A reduction in the rate of exchange between domains due to slower diffusion with decreased temperature may be responsible. The observation of a separate NMR signal from each domain for PEPC-d_{31} in PEPC-d_{31}/SM/chol and for PDPC-d_{31} in PDPC-d_{31}/SM/chol means that the relative concentration of PUFA-containing phospholipids in the two domains can be evaluated. A similar calculation for POPC-d_{31} in POPC-d_{31}/SM/chol was precluded. The spectrum at 30°C (Fig. 4 *c*, *left* and see Fig. S3) was of the same form as at 37°C (Fig. 2 *l*) and, consistent with fast exchange between domains remaining at lower temperature, a second spectral component did not appear.

We applied the FFT-dePaking algorithm (34) to determine the ratio of the quantity of PEPC-d_{31} and PDPC-d_{31} in PC-rich and SM-rich domains. By this numerical procedure, spectra characteristic of a membrane of single alignment were obtained. Fig. 4 (and see Fig. S4) illustrates that the powder patterns producing the two methyl peaks in the conventional spectra for PEPC-d_{31}/SM/chol (Fig. 4 *a*, *left*) become resolved as a pair of doublets (identified by *arrows*) in the dePaked spectra (Fig. 4 *a*, *right*). The ratio of the integrated intensity of inner and outer peaks, corresponding to the ratio of the amount of PEPC-d_{31} in the less-ordered PC-rich and more-ordered SM-rich domains, was then estimated to be 3:2 assuming a Lorentzian fit that is shown in the inset. Most of the EPA-containing PC

forms a more-disordered domain, whereas a smaller fraction (40%) incorporates into the SM-rich domain. By contrast, a ratio of 1:3 for the integrated intensity of the inner and outer peaks was determined when the pair of overlapping doublets (identified by *arrows*, and also see Fig. S4) in the dePaked spectrum for PDPC-d_{31}/SM/chol (Fig. 4 *b*, *right*) was analyzed. Although a more-disordered DHA-rich domain is formed, the majority (75%) of the DHA-containing PC is found to infiltrate into the more-ordered SM-rich (raftlike) domain. This remarkable finding is contrary to the propensity to segregate into DHA-rich/chol-poor (nonraft) domains identified in our previously published experiments on PDPE/SM/chol mixtures (16–18).

It should be understood that our estimate for the relative amount of PUFA-containing PC in each domain is approximate. The complexity of spectra meant that an analysis of the entire lineshape, which would be ideal, was not feasible. Instead, we focused upon the comparatively well-resolved signals attributed to terminal methyl groups. A potential problem with this approach is the possibility that a methylene group, rather than the terminal methyl group in a more-ordered domain, is responsible for the second innermost doublet in the dePaked spectrum for either PEPC-d_{31}/SM/chol (Fig. 4 *a*) or PDPC-d_{31}/SM/chol (Fig. 4 *b*). This possibility is discounted because a substantially greater differential in spitting with respect to the innermost doublet would be expected for a methylene group in the lower portion of a chain where order rapidly decreases toward the terminal methyl end.

The appearance of a minor spectral artifact at twice the frequency of the true signal after application of the FFT dePaking procedure (34) is another potential problem. A pair of small satellite peaks either side of the innermost doublet is an example of the artifact (Fig. 4 *c*) that, dependent upon the disposition of signals, can affect the analysis made here. The dePaked spectrum for PEPC-d_{31}/SM/chol (Fig. 4 *a*) is a worst case. There the artifact associated with the innermost doublet that we attribute to the terminal methyl group on PEPC-d_{31} in a less-ordered PC-rich domain lies buried underneath the second innermost doublet that we assign to the terminal methyl group on PEPC-d_{31} in a more-ordered SM-rich domain. A slight overestimation of PEPC-d_{31} found in the raftlike domain results. The situation is less severe with the dePaked spectrum for PDPC-d_{31}/SM/chol (Fig. 4 *b*). In this case, the artifact accompanying the innermost doublet assigned to PDPC-d_{31} in a less-ordered PC-rich domain falls just outside the second innermost doublet attributed to PDPC-d_{31} in a more-ordered SM-rich domain and is too small to be discerned.

How PDPE-d_{31} distributes between PE-rich and SM-rich domains in a PDPE-d_{31}/SM/chol (1:1:1 mol) membrane could not be quantified in our earlier NMR work because, as discussed above, only a single component spectrum was observed (17). Preferential segregation of PDPE-d_{31} into PE-rich/chol-poor domains was inferred from the relatively small increase in average order parameter registered by PDPE-d_{31} when chol was added to the PDPE-d_{31}/SM 1:1 mol mixture. In support of this interpretation, detergent extraction experiments conducted on PDPE/SM/chol (1:1:1 mol) showed that <30% PDPE was present in DRM where >90% SM and chol was found (17). A reduction in the amount of DHA-containing phospholipid that incorporates into SM-rich/chol-rich domains is implied, therefore, for PDPE compared to PDPC. The reduced affinity that PE has for chol compared to PC offers an explanation for this difference (14,15). We speculate that the uptake of DHA into lipid rafts within biological membranes may be dependent upon the lipid species into which the PUFA incorporates.

Because our ^{2}H-NMR experiments demonstrate that PDPC incorporates into SM/chol-rich (raft) domains to a greater extent than PEPC, we tested whether there is a difference in the incorporation of EPA and DHA in cells. DRM (rafts) and DSM (nonrafts) were isolated from EL4 cells in the presence of cold Triton X-100. It is acknowledged that the detergent produces artifacts (51). Nevertheless, this widely used method is a valuable screen with accepted utility as a predictive tool (10,52). Fig. S1 compares the uptake of EPA versus DHA, relative to a bovine serum albumin control, into EL4 cells. The data substantiate n-3 PUFA can be taken up into the DRM (raft) (see Fig. S1, *top panel*) as well as the DSM (nonraft) (see Fig. S1, *bottom panel*) fraction of a biological membrane. Indeed, ~30% of the uptake of EPA or DHA into EL4 cells was seen to be into DRM in earlier work (22). The complexity of cellular metabolism should be borne in mind here, because significant changes were detected in the levels of other fatty acids. Although the amount of DHA substantially exceeds the amount of EPA measured in both fractions, preferential incorporation of DHA cannot be inferred because the lower level of EPA comes at the expense of conversion to its elongation product DPA (40).

Biological implications

The data presented here agree with several cell culture and animal studies that show n-3 PUFA can directly infiltrate DRM, potentially impacting downstream cell signaling (21–23,41,53). In whole animals, we and others have established by a combination of imaging and lipidomic methods that n-3 PUFA disrupt lipid raft clustering in EL4 and primary B and T cells (21,23,53). By showing that DHA incorporates into raftlike domains more than EPA, the results obtained on model membranes in this work advance the field by providing evidence that DHA will be more effective than EPA in modifying lipid raft organization. This observation is highly consistent with our recent studies in which treatment of EL4 cells with DHA, but not EPA, was found to perturb the clustering and size of cholera-toxin induced lipid raft clusters (21).

Considerable controversy remains on how n-3 PUFA affect the spatial organization of lipid rafts. A primary issue is whether n-3 PUFA disrupt lipid rafts or make them more ordered. On the one hand, Kim et al. (23) proposed that n-3 PUFA can make raft domains more ordered. Using generalized polarization microscopy, these investigators reported that synapse lipid rafts of $CD4^+$ T cells from *fat-1* transgenic mice, which have high endogenous levels of n-3 PUFA, demonstrate increased order. Zech et al. (41), on the other hand, found that n-3 PUFA treatment of Jurkat T cells significantly disrupted raft organization as determined with lipidomics and polarization imaging. The difference between systems (in vitro versus ex vivo) was offered as an explanation (54).

Our work has the potential to explain the apparent discrepancy at a molecular level. The differential in segregation between raft and nonraft domains revealed for EPA and DHA suggest that the levels of these n-3 PUFA could determine impact on lipid raft organization. For instance, it is possible that EPA-containing phospholipids upon forming nonraft domains may redistribute chol molecules toward rafts to make them more ordered within the synapse. In contrast, DHA-containing phospholipids may make rafts more disordered and could have the opposite effect on rafts by forcing chol molecules out of rafts into nonraft regions. Clearly, more data are needed on the model membrane and cellular systems to establish a complete understanding of how EPA and DHA serve to modify membrane domain organization.

SUPPORTING MATERIAL

Additional experimental methods, one table, four figures, and reference (55) are available at http://www.biophysj.org/biophysj/supplemental/S0006-3495(12)00672-8.

This work was supported in part by a grant from the National Institutes of Health (No. R15AT006122 to S.R.S.).

REFERENCES

1. Calder, P. C., and P. Yaqoob. 2009. Omega-3 polyunsaturated fatty acids and human health outcomes. *Biofactors.* 35:266–272.
2. Chapkin, R. S., W. Kim, …, D. N. McMurray. 2009. Dietary docosahexaenoic and eicosapentaenoic acid: emerging mediators of inflammation. *Prostaglandins Leukot. Essent. Fatty Acids.* 81:187–191.
3. Fetterman, Jr., J. W., and M. M. Zdanowicz. 2009. Therapeutic potential of n-3 polyunsaturated fatty acids in disease. *Am. J. Health Syst. Pharm.* 66:1169–1179.
4. Harris, W. S., D. Mozaffarian, …, J. Whelan. 2009. Towards establishing dietary reference intakes for eicosapentaenoic and docosahexaenoic acids. *J. Nutr.* 139:804S–819S.
5. Stillwell, W., and S. R. Wassall. 2003. Docosahexaenoic acid: membrane properties of a unique fatty acid. *Chem. Phys. Lipids.* 126:1–27.
6. Wassall, S. R., and W. Stillwell. 2008. Docosahexaenoic acid domains: the ultimate non-raft membrane domain. *Chem. Phys. Lipids.* 153: 57–63.
7. Yaqoob, P., and S. R. Shaikh. 2010. The nutritional and clinical significance of lipid rafts. *Curr. Opin. Clin. Nutr. Metab. Care.* 13:156–166.
8. Levental, I., M. Grzybek, and K. Simons. 2010. Greasing their way: lipid modifications determine protein association with membrane rafts. *Biochemistry.* 49:6305–6316.
9. Pike, L. J. 2006. Rafts defined: a report on the Keystone symposium on lipid rafts and cell function. *J. Lipid Res.* 47:1597–1598.
10. Lingwood, D., and K. Simons. 2010. Lipid rafts as a membrane-organizing principle. *Science.* 327:46–50.
11. Bartels, T., R. S. Lankalapalli, …, M. F. Brown. 2008. Raftlike mixtures of sphingomyelin and cholesterol investigated by solid-state ^{2}H NMR spectroscopy. *J. Am. Chem. Soc.* 130:14521–14532.
12. Feller, S. E. 2008. Acyl chain conformations in phospholipid bilayers: a comparative study of docosahexaenoic acid and saturated fatty acids. *Chem. Phys. Lipids.* 153:76–80.
13. Soubias, O., and K. Gawrisch. 2007. Docosahexaenoyl chains isomerize on the sub-nanosecond time scale. *J. Am. Chem. Soc.* 129:6678–6679.
14. Shaikh, S. R., V. Cherezov, …, S. R. Wassall. 2006. Molecular organization of cholesterol in unsaturated phosphatidylethanolamines: x-ray diffraction and solid state ^{2}H NMR reveal differences with phosphatidylcholines. *J. Am. Chem. Soc.* 128:5375–5383.
15. Niu, S. L., and B. J. Litman. 2002. Determination of membrane cholesterol partition coefficient using a lipid vesicle-cyclodextrin binary system: effect of phospholipid acyl chain unsaturation and headgroup composition. *Biophys. J.* 83:3408–3415.
16. Shaikh, S. R., M. R. Brzustowicz, …, S. R. Wassall. 2002. Monounsaturated PE does not phase-separate from the lipid raft molecules sphingomyelin and cholesterol: role for polyunsaturation? *Biochemistry.* 41:10593–10602.
17. Shaikh, S. R., A. C. Dumaual, …, S. R. Wassall. 2004. Oleic and docosahexaenoic acid differentially phase separate from lipid raft molecules: a comparative NMR, DSC, AFM, and detergent extraction study. *Biophys. J.* 87:1752–1766.
18. Soni, S. P., D. S. LoCascio, …, S. R. Wassall. 2008. Docosahexaenoic acid enhances segregation of lipids between raft and non-raft domains: ^{2}H NMR study. *Biophys. J.* 95:203–214.
19. Kučerka, N., D. Marquardt, …, J. Katsaras. 2010. Cholesterol in bilayers with PUFA chains: doping with DMPC or POPC results in sterol reorientation and membrane-domain formation. *Biochemistry.* 49:7485–7493.
20. Wassall, S. R., and W. Stillwell. 2009. Polyunsaturated fatty acid-cholesterol interactions: domain formation in membranes. *Biochim. Biophys. Acta.* 1788:24–32.
21. Fan, Y. Y., D. N. McMurray, …, R. S. Chapkin. 2003. Dietary (n-3) polyunsaturated fatty acids remodel mouse T-cell lipid rafts. *J. Nutr.* 133:1913–1920.
22. Shaikh, S. R., B. D. Rockett, …, K. Carraway. 2009. Docosahexaenoic acid modifies the clustering and size of lipid rafts and the lateral organization and surface expression of MHC class I of EL4 cells. *J. Nutr.* 139:1632–1639.
23. Kim, W., Y. Y. Fan, …, R. S. Chapkin. 2008. n-3 polyunsaturated fatty acids suppress the localization and activation of signaling proteins at the immunological synapse in murine CD^{4+} T cells by affecting lipid raft formation. *J. Immunol.* 181:6236–6243.
24. Shaikh, S. R. 2010. Diet-induced docosahexaenoic acid non-raft domains and lymphocyte function. *Prostaglandins Leukot. Essent. Fatty Acids.* 28:159–164.
25. Salem, Jr., N., H. Y. Kim, and J. A. Yergey. 1986. Docosahexaenoic acid: membrane function and metabolism. *In* The Health Effects of Polyunsaturated Fatty Acids in Seafoods. A. P. Simopoulos, R. R. Kifer, and R. Martin, editors. Academic Press, New York. 317–363.
26. Kris-Etherton, P. M., W. S. Harris, L. J. Appel; Nutrition Committee. 2003. Fish consumption, fish oil, omega-3 fatty acids, and cardiovascular disease. *Arterioscler. Thromb. Vasc. Biol.* 23:e20–e30.

27. Mori, T. A., D. Q. Bao, …, L. J. Beilin. 1999. Docosahexaenoic acid but not eicosapentaenoic acid lowers ambulatory blood pressure and heart rate in humans. *Hypertension.* 34:253–260.

28. Park, Y., and W. Harris. 2002. EPA, but not DHA, decreases mean platelet volume in normal subjects. *Lipids.* 37:941–946.

29. Vemuri, M., D. S. Kelley, …, G. Bartolini. 2007. Docosahexaenoic acid (DHA) but not eicosapentaenoic acid (EPA) prevents *trans*-10, *cis*-12 conjugated linoleic acid (CLA)-induced insulin resistance in mice. *Metab. Syndr. Relat. Disord.* 5:315–322.

30. Shaikh, S. R., D. S. Locascio, …, W. Stillwell. 2009. Oleic- and docosahexaenoic acid-containing phosphatidylethanolamines differentially phase separate from sphingomyelin. *Biochim. Biophys. Acta.* 1788:2421–2426.

31. Soni, S. P., J. A. Ward, …, S. R. Wassall. 2009. Effect of *trans* unsaturation on molecular organization in a phospholipid membrane. *Biochemistry.* 48:11097–11107.

32. Davis, J. H., K. R. Jeffrey, …, T. P. Higgs. 1976. Quadrupolar echo deuteron magnetic resonance spectroscopy in ordered hydrocarbon chains. *Chem. Phys. Lett.* 42:390–394.

33. Davis, J. H. 1983. The description of membrane lipid conformation, order and dynamics by ^{2}H-NMR. *Biochim. Biophys. Acta.* 737: 117–171.

34. McCabe, M. A., and S. R. Wassall. 1997. Rapid deconvolution of NMR powder spectra by weighted fast Fourier transformation. *Solid State Nucl. Magn. Reson.* 10:53–61.

35. Barry, J. A., T. P. Trouard, …, M. F. Brown. 1991. Low-temperature ^{2}H NMR spectroscopy of phospholipid bilayers containing docosahexaenoyl (22:6 ω3) chains. *Biochemistry.* 30:8386–8394.

36. Wassall, S. R., M. A. McCabe, …, S. E. Feller. 2010. Solid-state ^{2}H NMR and MD simulations of positional isomers of a monounsaturated phospholipid membrane: structural implications of double bond location. *J. Phys. Chem. B.* 114:11474–11483.

37. Niebylski, C. D., and N. Salem, Jr. 1994. A calorimetric investigation of a series of mixed-chain polyunsaturated phosphatidylcholines: effect of *sn*-2 chain length and degree of unsaturation. *Biophys. J.* 67: 2387–2393.

38. Bunge, A., P. Müller, …, D. Huster. 2008. Characterization of the ternary mixture of sphingomyelin, POPC, and cholesterol: support for an inhomogeneous lipid distribution at high temperatures. *Biophys. J.* 94:2680–2690.

39. Ausili, A., A. Torrecillas, …, J. C. Gómez-Fernández. 2008. Edelfosine is incorporated into rafts and alters their organization. *J. Phys. Chem. B.* 112:11643–11654.

40. Kaur, G., A. J. Sinclair, …, N. Konstantopoulos. 2011. Docosahexaenoic acid (22:5n-3) down-regulates the expression of genes involved in fat synthesis in liver cells. *Prost. Leuk. Essent. Fatty Acids.* 85:155–161.

41. Zech, T., C. S. Ejsing, …, T. Harder. 2009. Accumulation of raft lipids in T-cell plasma membrane domains engaged in TCR signaling. *EMBO J.* 28:466–476.

42. Petrache, H. I., S. W. Dodd, and M. F. Brown. 2000. Area per lipid and acyl chain length distributions in fluid phosphatidylcholines determined by ^{2}H NMR spectroscopy. *Biophys. J.* 78:3172–3192.

43. Salmon, A., S. W. Dodd, …, M. F. Brown. 1987. Configurational statistics of acyl chains in polyunsaturated lipid bilayers from ^{2}H NMR. *J. Am. Chem. Soc.* 109:2600–2609.

44. Polozov, I. V., and K. Gawrisch. 2007. NMR detection of lipid domains. *Methods Mol. Biol.* 398:107–126.

45. Mihailescu, M., O. Soubias, …, K. Gawrisch. 2011. Structure and dynamics of cholesterol-containing polyunsaturated lipid membranes studied by neutron diffraction and NMR. *J. Membr. Biol.* 239:63–71.

46. Hsueh, Y.-W., M.-T. Chen, …, J. Thewalt. 2007. Ergosterol in POPC membranes: physical properties and comparison with structurally similar sterols. *Biophys. J.* 92:1606–1615.

47. Jackman, C. S., P. J. Davis, …, K. M. W. Keough. 1999. Effect of cholesterol on the chain-ordering transition of 1-palmitoyl-2-arachidonoyl phosphatidylcholine. *J. Phys. Chem. B.* 103:8830–8836.

48. Bloom, M., and J. Thewalt. 1994. Spectroscopic determination of lipid dynamics in membranes. *Chem. Phys. Lipids.* 73:27–38.

49. Filippov, A., G. Orädd, and G. Lindblom. 2006. Sphingomyelin structure influences the lateral diffusion and raft formation in lipid bilayers. *Biophys. J.* 90:2086–2092.

50. Shaikh, S. R., V. Cherezov, …, S. R. Wassall. 2003. Interaction of cholesterol with a docosahexaenoic acid-containing phosphatidylethanolamine. Trigger for microdomain formation? *Biochemistry.* 42:12028–12038.

51. Heerklotz, H. 2002. Triton promotes domain formation in lipid raft mixtures. *Biophys. J.* 83:2693–2701.

52. Edidin, M. 2003. The state of lipid rafts: from model membranes to cells. *Annu. Rev. Biophys. Biomol. Struct.* 32:257–283.

53. Rockett, B. D., A. Franklin, …, S. R. Shaikh. 2011. Membrane raft organization is more sensitive to disruption by (n-3) PUFA than nonraft organization in EL4 and B cells. *J. Nutr.* 141:1041–1048.

54. Kim, W., N. A. Khan, …, R. S. Chapkin. 2010. Regulatory activity of polyunsaturated fatty acids in T-cell signaling. *Prog. Lipid Res.* 49:250–261.

55. Rockett, B. D., M. Salameh, …, S. R. Shaikh. 2010. n-3 PUFA improves fatty acid composition, prevents palmitate-induced apoptosis, and differentially modifies B cell cytokine secretion in vitro and ex vivo. *J. Lipid Res.* 51:1284–1297.